HHS Public Access

Author manuscript

Brain Res. Author manuscript; available in PMC 2020 July 15.

Published in final edited form as:

Brain Res. 2019 July 15; 1715: 94–105. doi:10.1016/j.brainres.2019.03.029.

Antimycin A-induced mitochondrial dysfunction activates vagal sensory neurons via ROS-dependent activation of TRPA1 and ROS-independent activation of TRPV1

Katherine R Stanford[1], **Stephen H Hadley**[1], **Ivan Barannikov**[1], **Joanne M Ajmo**[1], **Parmvir K Bahia**[1], and **Thomas E Taylor-Clark**[1,*]

[1]Department of Molecular Pharmacology & Physiology, Morsani College of Medicine, University of South Florida, Tampa, FL, USA

Abstract

Inflammation causes activation of nociceptive sensory nerves, resulting in debilitating sensations and reflexes. Inflammation also induces mitochondrial dysfunction through multiple mechanisms. Sensory nerve terminals are densely packed with mitochondria, suggesting that mitochondrial signaling may play a role in inflammation-induced nociception. We have previously shown that agents that induce mitochondrial dysfunction, such as antimycin A, activate a subset of nociceptive vagal sensory nerves that express transient receptor potential (TRP) channels ankyrin 1 (A1) and vanilloid 1 (V1). However, the mechanisms underlying these responses are incompletely understood. Here, we studied the contribution of TRPA1, TRPV1 and reactive oxygen species (ROS) to antimycin A-induced vagal sensory nerve activation in dissociated neurons and at the sensory terminals of bronchopulmonary C-fibers. Nociceptive neurons were defined chemically and genetically. Antimycin A-evoked activation of vagal nociceptors in a Fura2 Ca^{2+} assay correlated with TRPV1 responses compared to TRPA1 responses. Nociceptor activation was dependent on both TRP channels, with TRPV1 predominating in a majority of responding nociceptors and TRPA1 predominating only in nociceptors with the greatest responses. Surprisingly, both TRPA1 and TRPV1 were activated by H_2O_2 when expressed in HEK293. Nevertheless, targeting ROS had no effect of antimycin A-evoked TRPV1 activation in either HEK293 or vagal neurons. In contrast, targeting ROS inhibited antimycin A-evoked TRPA1 activation in HEK293, vagal neurons and bronchopulmonary C-fibers, and a ROS-insensitive TRPA1 mutant was completely insensitive to antimycin A. We therefore conclude that mitochondrial dysfunction activates vagal nociceptors by ROS-dependent (TRPA1) and ROS-independent (TRPV1) mechanisms.

Keywords

Nociceptor; C-fiber; TRPA1; TRPV1; mitochondria; reactive oxygen species; vagal; antimycin A

*Corresponding Author: ttaylorc@health.usf.edu, 12901 Bruce B Downs Blvd, University of South Florida, Tampa, FL, 33612.

1. Introduction

Vagal sensory nerves innervate organs throughout the thoracic and abdominal compartments, and their activation by local stimuli regulate reflexes that maintain homeostasis or protect the organ. One major subset of vagal sensory nerves, termed “nociceptors”, is activated by a variety of noxious stimuli, including excessive temperature, mechanical force, pH, inflammatory mediators and irritants. This broad sensitivity is due to the expression of multiple receptors such as the allyl isothiocyanate (AITC)-sensitive transient receptor potential (TRP) ankyrin 1 (A1) channel and the capsaicin-sensitive TRP vanilloid 1 (V1) channel (Jones et al., 2005; Mishra et al., 2011; Patapoutian et al., 2009; Trankner et al., 2014). Although activation of these nociceptive sensory nerves initiates protective reflexes, aberrant activation is thought to play a primary role in the chronic initiation of uncontrolled defensive reflexes, sensations and behaviors in inflammatory diseases including asthma, irritable bowel disease, gastroesophageal reflux disorder and colitis.

Sensory nerve terminals are densely packed with mitochondria (Hung et al., 1973; von During and Andres, 1988). In addition to the production of ATP through oxidative phosphorylation, mitochondria contribute to cellular signaling processes via many mechanisms including the production of reactive oxygen species (ROS) and the buffering of cytosolic Ca^{2+} (Gunter et al., 2004; Stowe and Camara, 2009). Inflammatory signaling, such as tumor necrosis factor α, neurotrophins, toll-like receptors and transforming factor β, causes mitochondrial dysfunction and the production of ROS (Corda et al., 2001; Michaeloudes et al., 2010; Pehar et al., 2007; West et al., 2011). This inflammation-associated mitochondrial ROS production is linked to the inhibition of the protein complexes that make up the mitochondrial electron transport chain (mETC). While this can cause apoptosis, partial inhibition of mETC produces significant ROS production and mitochondrial depolarization without leading to cellular death (Brunelle et al., 2005).

We have previously shown that inhibition of mETC complex III with antimycin A causes the activation of nociceptive vagal sensory nerves, which is reduced by the pharmacological inhibition or the genetic knockout of either TRPA1 or TRPV1 (Nesuashvili et al., 2013). Furthermore, antimycin A causes activation of both TRPA1 and TRPV1 when expressed in HEK293 cells. TRPA1 is directly gated by ROS and other electrophilic compounds produced by oxidative stress (e.g. 4-hydroxynonenal) (Andersson et al., 2008; Sawada et al., 2008; Taylor-Clark et al., 2008a) suggesting that ROS may mediate the antimycin A-evoked TRPA1 activation. Our previous data demonstrated that a combination of ROS scavengers, MnTMPyP and tempol, inhibited the initial antimycin A-evoked activation of TRPA1-expressing HEK293 by 75%, although eventually antimycin A evoked strong TRPA1 activation (Nesuashvili et al., 2013). We have also reported that despite antimycin A-induced neuronal activation correlating with mitochondrial ROS production, some TRPA1-expressing neurons which had a substantial increase in mitochondrial ROS were not activated (Stanford and Taylor-Clark, 2018). In addition, some nociceptive neurons were strongly activated in the absence of any measurable mitochondrial ROS production. As such, it is unclear what contribution ROS makes to the antimycin A-evoked activation of the polymodal receptors TRPA1 and TRPV1 in vagal neurons.

Our previous studies of antimycin A-evoked Ca^{2+} fluxes presented data from nociceptors defined by their responsiveness to AITC and capsaicin (TRPA1 and TRPV1 agonists, respectively) (Nesuashvili et al., 2013). These criteria are affected by TRP channel inhibition/knockout, thus the non-responsive nociceptor populations were likely underreported. Given that TRPV1 expression is more widely expressed in vagal nociceptors compared to TRPA1 (Nassenstein et al., 2008; Nesuashvili et al., 2013), the role of TRPV1 may have be underreported.

Given these previous findings there is considerable uncertainty about the contribution of TRPA1, TRPV1 and ROS to the activation of vagal nociceptive neurons. Here we show using a comprehensive combinatory approach in genetically-defined nociceptive populations with both TRP channel inhibition and knockout that antimycin A causes Ca^{2+} fluxes in vagal sensory neurons via TRPA1, TRPV1 and another unidentified Gd^{3+}-sensitive Ca^{2+} channel. Surprisingly, antimycin A-evoked populational Ca^{2+} responses correlate with capsaicin responses compared to AITC responses and the inhibition/knockout of TRPV1 has a greater effect on the antimycin A-evoked populational responses. Nevertheless, TRPA1 plays a predominant role in the activation of a subset of vagal nociceptors with the greatest antimycin A-evoked responses. We also show that although H_2O_2 activates both TRPA1- and TRPV1-expressing HEK293, the antimycin A-evoked activation of heterologously-expressed TRPA1 is exclusively ROS-mediated whereas TRPV1 activation is ROS-independent. Finally, we show that, in both dissociated vagal neurons and at the peripheral terminals of bronchopulmonary vagal afferents, antimycin-evoked activation of nociceptors via TRPA1 is ROS-mediated, but the TRPV1-mediated mechanism is ROS-independent. These novel findings highlight the limited role that ROS and TRPA1 play in the activation of vagal nociceptors during mitochondrial dysfunction.

2. Results

2.1 Characterization of vagal sensory neurons from $TRPV1^{Cre/+}$/ROSA26-$tdTomato^{fl/+}$ mice

Previous studies have shown that mitochondrial modulators selectively activate a proportion of nociceptive vagal sensory neurons (Nesuashvili et al., 2013; Stanford and Taylor-Clark, 2018). To aid the identification of nociceptive neurons in our studies, we chose to use a cre/lox approach with $TRPV1^{Cre}$ (Cavanaugh et al., 2011) and a floxed tdTomato reporter mouse, thereby identifying TRPV1-lineage cells. We first characterized the responses of dissociated vagal sensory neurons from $TRPV1^{Cre/+}$/ROSA26-$tdTomato^{fl/+}$ mice to AITC (100μM, TRPA1 agonist) and capsaicin (1μM, TRPV1 agonist) in a Fura 2AM Ca^{2+} assay. In general, both AITC and capsaicin caused an increase in $[Ca^{2+}]_i$ in tdTomato-expressing neurons but not in neurons that lacked tdTomato, consistent with the selective expression of TRPA1 and TRPV1 in TRPV1-lineage cells (Fig 1). However, only 68 out of 89 tdTomato-expressing neurons responded to at least one of the TRP agonists. Although it is likely that at some point in development these neurons were sensitive to nociceptive stimuli, the physiological function of these irritant-insensitive TRPV1-lineage neurons is unclear. Furthermore, of the 28 neurons that did not express tdTomato, 5 responded to at least one of the TRP agonists. As such, we defined vagal nociceptor as a neuron that fulfilled at least one

of the following criteria: (1) positive expression of tdTomato, (2) responsiveness to at least one of the TRP agonists. Thus, in these preliminary studies 80% of vagal neurons were identified as nociceptive.

2.2 Antimycin A activates a subset of vagal sensory neurons via gating of TRPA1 and TRPV1

Using Fura 2AM Ca^{2+} imaging, we determined the response of dissociated vagal sensory neurons from $TRPV1^{Cre/+}$/ROSA26-$tdTomato^{fl/+}$ mice to antimycin A (10 μM, complex III inhibitor), AITC (100 μM) and capsaicin (1 μM). As before, neurons were characterized by their responsiveness to AITC and capsaicin and their expression of tdTomato in order to ascertain their nociceptive status. In total, 402 out of 486 vagal neurons (83%) were identified as nociceptive. Consistent with previous findings (Nesuashvili et al., 2013; Stanford and Taylor-Clark, 2018), antimycin A caused a greater increase in $[Ca^{2+}]_i$ in nociceptive neurons than in non-nociceptive neurons ($p<0.05$, Fig 2A and B). Interestingly, significant antimycin A-evoked responses only occurred in a subset (222/402) of nociceptive neurons (Fig 2C) – these were termed 'responding' nociceptors (see methods for definition). Surprisingly, antimycin A-evoked responses had a stronger correlation with capsaicin responses ($R^2 = 0.48$, $p<0.001$) than AITC responses ($R^2 = 0.23$, $p<0.001$), and very few neurons that were activated by AITC but not capsaicin had robust antimycin A-evoked responses (Fig 2C). There were no differences between the Ca^{2+} responses to antimycin A in 'non-responding' nociceptors and in nonnociceptive neurons ($p>0.05$, Fig 2A and B).

Antimycin A-evoked increases in $[Ca^{2+}]_i$ were abolished by pretreatment of vagal neurons (n=57) with a combination of ruthenium red (30 μM) and Gd^{3+} (300 μM)(Fig 2B). Pretreatment of vagal neurons with ruthenium red alone (n=117) reduced antimycin A-evoked Ca^{2+} responses compared to non-nociceptive neurons in control conditions (0.11 ± 0.01 vs. 0.20 ± 0.01 (n=84), $p<0.05$). Nevertheless, the residual antimycin A-evoked responses during treatment with ruthenium red alone was significantly greater than during treatment with the combination of ruthenium and Gd^{3+} ($p<0.05$). Ruthenium red and Gd^{3+} are blockers of multiple Ca^{2+} permeable channels including TRPA1, TRPV1 and TRPM7 (Harding et al., 2018; Wu et al., 2010). TRPM7 is expressed in all sensory nerve subtypes (Usoskin et al., 2015; Wang et al., 2017) and is reported to be activated by ROS (Yoshida et al., 2006). We hypothesized that TRPM7 was responsible for the Gd^{3+}-sensitive antimycin-evoked Ca^{2+} fluxes in non-nociceptive neurons. Pretreatment of vagal neurons from $TRPV1^{Cre/+}$/ROSA26-$tdTomato^{fl/+}$ mice with the TRPM7 inhibitor NS8593 (30 μM) (Chubanov et al., 2012) had no effect on the antimycin A-evoked responses in the non-nociceptive population (0.22 ± 0.02 (n=31) vs. 0.20 ± 0.01 (n=84), $p>0.05$), indicating that TRPM7 was not involved. Nevertheless, antimycin A-evoked responses in the entire vagal population were eliminated by buffering extracellular $[Ca^{2+}]$ to 100nM (n=53)(Fig 2B), thus confirming the role of Ca^{2+} influx.

Using a combination of pharmacological and genetic strategies we determined the contribution of TRPA1 and TRPV1 in the response of vagal neurons to antimycin A (Figs 3 and 4). $TRPV1^{Cre/+}$/ROSA26-$tdTomato^{fl/+}$ neurons (n=486) were compared with $TRPV1^{Cre/+}$/ROSA26-$tdTomato^{fl/+}$ neurons pretreated with the TRPA1 inhibitor A967079

(5 μM) and/or the TRPV1 inhibitor iodoresiniferatoxin (I-RTX, 500 nM), and also compared with TRPA1$^{-/-}$ neurons or TRPV1$^{-/-}$ neurons with or without complementary TRP inhibitors. Given that vagal neurons are heterogenous and that antimycin A-evoked responses are restricted to an undefined subgroup of nociceptors, the responses were analyzed in four separate ways: mean $[Ca^{2+}]_i$ responses of all neurons (Fig 3 A–D), the % of neurons responding (Fig 3E), mean $[Ca^{2+}]_i$ responses of 'responding' neurons (Fig 3F), and histograms of individual $[Ca^{2+}]_i$ responses (Fig 4). Preliminary studies demonstrated that 50nM A967079 reduced AITC-evoked responses by 85% (n=28, $p<0.05$, data not shown) and previous studies (Nesuashvili et al., 2013; Taylor-Clark et al., 2008a) have demonstrated complete inhibition of capsaicin-evoked responses in vagal neurons by I-RTX. While A967079 inhibition is reversible, under these conditions I-RTX inhibition is not reversible.

Inhibition of TRPA1 with A967079 (n=137) decreased the mean antimycin A-evoked $[Ca^{2+}]_i$ response ($p<0.05$, Fig 3A and D), but had no effect on the % of neurons responding ($p>0.05$, Fig 3E). Genetic ablation of TRPA1 (n=782) reduced the mean antimycin A-evoked $[Ca^{2+}]_i$ response but this was not significantly different to either control neurons or neurons treated with A967079 ($p>0.05$, Fig 3A and D). Consistent with the TRPA1 inhibitor data, the % of neurons responding to antimycin was not different in TRPA1$^{-/-}$ neurons ($p>0.05$, Fig 3E). Whereas, inhibition of TRPV1 with I-RTX (n=292) or genetic ablation of TRPV1 (n=221) both decreased the mean antimycin A-evoked $[Ca^{2+}]_i$ response ($p<0.05$, Fig 3B and D), and reduced the % of neurons responding ($p<0.05$, Fig 3E). Thus, targeting either TRPA1 or TRPV1 decreased antimycin A-induced populational responses. We used three anti-TRP combinations to simultaneously inhibit TRPA1 and TRPV1 function: TRPV1$^{Cre/+}$/ROSA26-tdTomato$^{fl/+}$ neurons pretreated with both A967079 and I-RTX (n=196), TRPA1$^{-/-}$ neurons pretreated with I-RTX (n=168), and TRPV1$^{-/-}$ neurons pretreated with A967079 (n=168). All three combinations further decreased the mean antimycin A-evoked $[Ca^{2+}]_i$ response compared to targeting a single TRP channel ($p<0.05$, Fig 3C and D). Virtually no neurons were classified as 'responders' with all three combinations ($p>0.05$, Fig 3E). There were no significant differences between antimycin A-evoked Ca^{2+} responses in the non-nociceptive population under control conditions and the total vagal population under conditions in which both TRPA1 and TRPV1 were inhibited/targeted. It is likely therefore that the Gd^{3+}-sensitive mechanism responsible for antimycin-evoked Ca^{2+} influx in non-nociceptive neurons is also present in the nociceptive population.

Despite the fact that inhibition or genetic ablation of TRPV1 reduced the mean antimycin A-evoked $[Ca^{2+}]_i$ response of the total neuronal population (Fig 3D), targeting TRPV1 alone had no effect on the mean $[Ca^{2+}]_i$ response of 'responding' neurons (Fig 3F). Whereas both inhibition and genetic ablation of TRPA1 reduced the mean $[Ca^{2+}]_i$ responses of 'responding' neurons ($p<0.05$, Fig 3F). These observations suggest that TRPA1 and TRPV1 contribute to vagal nociceptor activation in distinct ways. Clearly, TRPV1 inhibition/knockout reduced the antimycin A-evoked responses of approximately 25% of vagal neurons to levels equivalent to 'non-responding'/non-nociceptive neurons. Yet, the remaining 'responders' under conditions of TRPV1 inhibition/knockout have disproportionately greater Ca^{2+} responses than the overall 'responding' nociceptor population under control conditions, thus resulting in the apparent lack of effect of TRPV1 inhibition/knockout on the magnitude of 'responders'. This can be visualized in histograms

of the antimycin A-evoked responses under each condition (Fig 4). Under control conditions 82 of 180 responders (46%) had an antimycin A-evoked Ca^{2+} response of >0.9 (Fig 4A). During treatment with TRPV1 inhibitor I-RTX 21 of 35 responders (60%) had an antimycin A-evoked Ca^{2+} response of >0.9 (Fig 4C) and, similarly, 17 of 31 (55%) of responders from TRPV1$^{-/-}$ ganglia had an antimycin A-evoked Ca^{2+} response of >0.9 (Fig 4G). Whereas during treatment with TRPA1 inhibitor A967079 11 of 47 responders (23%) had an antimycin A-evoked Ca^{2+} response of >0.9 (Fig 4B), which is significantly less than control ($p<0.05$). Similarly, 111 of 311 responders (36%) from TRPA1$^{-/-}$ ganglia had an antimycin A-evoked Ca^{2+} response of >0.9 (Fig 4E), which is less than control but this did not reach significance ($p=0.079$). Thus, TRPV1 is the predominant contributor to antimycin A-evoked Ca^{2+} responses in the overall nociceptor population but TRPA1 is the predominant mechanism in 'responders' with the greatest antimycin A-evoked responses. Importantly, combined targeting of TRPA1 and TRPV1 reduced vagal neuron responses to background responses observed in 'non-responding' nociceptors and non-nociceptors (Fig 4 D, F and H).

2.3 Contribution of oxidative stress to antimycin A-induced $[Ca^{2+}]_i$ responses

Antimycin A causes mitochondrial ROS production in vagal sensory neurons (Stanford and Taylor-Clark, 2018). Given that ROS and products of oxidative stress are activators of TRPA1 (Andersson et al., 2008; Sawada et al., 2008; Taylor-Clark et al., 2008a), we hypothesized that antimycin A-induced TRPA1 activation would be downstream of ROS production. In our previous studies, antimycin A-induced activation of TRPA1-expressing HEK293 was initially inhibited by a combination of ROS scavengers by 75%, although eventually antimycin A evoked strong TRPA1 activation (Nesuashvili et al., 2013). Given that TRPA1 is a polymodal channel activated by multiple mechanisms (Bautista et al., 2006; Jordt et al., 2004; Wu et al., 2010) it is presently unclear if ROS are solely responsible for antimycin A-evoked TRPA1 activation. TRPV1 has been reported to be insensitive to micromolar concentrations of ROS (Andersson et al., 2008). Thus we hypothesized that ROS would not play a role in antimycin A-induced TRPV1 activation.

We first addressed our hypotheses using heterologous expression of hTRPA1 and hTRPV1 in HEK293 cells. As expected, H_2O_2 (100 μM) activated TRPA1 ($p<0.05$, Fig 5A), with 53 out of 62 TRPA1-expressing HEK293 having a Ca^{2+} response >0.4 (Fig 5C), whereas H_2O_2 had little effect on non-transfected HEK293 ($n=95$, Fig 5A and B). Surprisingly, H_2O_2 also activated TRPV1 ($p<0.05$, Fig 5A), although only a small subset of TRPV1-expressing HEK293 (60 out of 212) had a Ca^{2+} response >0.4. Overall, H_2O_2 caused greater Ca^{2+} fluxes in TRPA1-expressing HEK293 compared to TRPV1-expressing HEK293 ($p<0.05$). Nevertheless, analysis of HEK293 with Ca^{2+} responses >0.4 shows that TRPV1-expressing HEK293 'responders' have greater H_2O_2-evoked responses than TRPA1-expressing HEK293 'responders' (1.54 ± 0.07 vs. 1.00 ± 0.04, $p<0.05$).

Antimycin A (10 μM) caused an increase in $[Ca^{2+}]_i$ in TRPA1-HEK293 ($n=658$) and TRPV1-HEK293 ($n=703$), but had little effect on non-transfected HEK293 cells ($n=112$) (Fig 5E–J). Pretreatment with the reducing agent dithiothreitol (DTT, 100 μM) reduced the antimycin A-induced activation of TRPA1 ($n=579$) but not that of TRPV1 ($n=564$)(Fig 5E, F, J). To confirm the role of oxidative stress in TRPA1 activation, we used the ROS-

insensitive K620A mutant of hTRPA1 (Bahia et al., 2016). This mutant fails to bind electrophiles and is not activated by ROS and other electrophiles but can be activated by thymol. Antimycin A (10 μM) failed to activate TRPA1-K620A (n=74, $p<0.05$ compared to wild-type TRPA1), which nonetheless was activated by thymol (200 μM)(Fig 5K, L).

We then tested the role of oxidative stress in the antimycin A-induced activation of TRPA1 and TRPV1 in dissociated mouse vagal neurons. Vagal neurons from TRPV1$^{-/-}$ mice and TRPA1$^{-/-}$ mice were treated with antimycin A in the presence of vehicle (0.1% ethanol) or a combination of ROS scavengers: MnTMPyP (50 μM) and tempol (100 μM). As before, antimycin A evoked an increase in $[Ca^{2+}]_i$ in vehicle-pretreated TRPV1$^{-/-}$ neurons (n=291) and TRPA1$^{-/-}$ neurons (n=168)(Fig 6). The antioxidant combination reduced the mean antimycin A-evoked $[Ca^{2+}]_i$ response of the total TRPV1$^{-/-}$ neuronal population (n=328) ($p<0.05$) and the mean antimycin A-evoked $[Ca^{2+}]_i$ response of 'responding' TRPV1$^{-/-}$ neurons ($p<0.05$) (Fig 6A). The antioxidant combination also appeared to reduce the % of TRPV1$^{-/-}$ neurons responding (Fig 6B) but this did not reach significance. Conversely, the antioxidant combination had no effect on the mean antimycin A-evoked $[Ca^{2+}]_i$ response of the total TRPA1$^{-/-}$ neuronal population (n=324)($p>0.05$), or on the mean antimycin A-evoked $[Ca^{2+}]_i$ response of 'responding' TRPA1$^{-/-}$ neurons ($p>0.05$) (Fig 6C), and had no effect on the % of TRPA1$^{-/-}$ neurons responding (Fig 6D). Thus, as with the heterologously expressed TRP channels, antimycin A-evoked TRPA1 in mouse vagal neurons was dependent on ROS, but TRPV1-mediated responses were independent of ROS.

2.4 Role of TRPs and oxidative stress in antimycin A-evoked activation of bronchopulmonary C-fibers

We studied the mechanisms underlying the antimycin A-evoked activation of sensory terminals innervating the bronchopulmonary tree using single fiber recordings in an ex vivo vagal-lung preparation (Nesuashvili et al., 2013). Individual vagal bronchopulmonary fibers were characterized by conduction velocity and responsivity to AITC (30 μM) and capsaicin (1 μM). Previous studies have shown that only slow bronchopulmonary C-fibers (<0.7 m/s) in the mouse respond to TRPA1 or TRPV1 (Kollarik et al., 2003; Nassenstein et al., 2008), thus only these fibers were studied. As expected, capsaicin activated all slow bronchopulmonary C-fibers from wild-type mice (peak discharge of 19.0±3.1 Hz), whereas AITC only activated 20 of 34 capsaicin-sensitive bronchopulmonary C-fibers (peak discharge of 13.7±0.9 Hz). Bronchopulmonary C-fibers sensitive to both AITC and capsaicin conducted action potentials significantly slower than fibers sensitive to only capsaicin (0.48±0.01 m/s vs. 0.54±0.02 m/s, $p<0.05$). Antimycin A (20 μM) evoked action potential discharge over a period of 600s from both AITC-sensitive and AITC-insensitive bronchopulmonary C-fibers from wild-type mice. Antimycin A activated all 20 AITC-sensitive bronchopulmonary C-fibers and activated 7 out of 14 AITC-insensitive bronchopulmonary C-fibers. Antimycin A-evoked significantly more action potentials from AITC-sensitive fibers than AITC-insensitive fibers ($p<0.05$)(Fig 7).

We studied the role of TRPA1 and TRPV1 in antimycin A-induced activation of bronchopulmonary C-fibers using a combination of genetic and pharmacological inhibition. Antimycin A evoked action potential discharge from 5 of 7 TRPA1$^{-/-}$ C-fibers, and the

firing was significantly reduced compared to wild-type fibers ($p<0.05$)(Fig 7). Pretreatment of TRPA1$^{-/-}$ C-fibers with the TRPV1 inhibitor I-RTX (1 μM, n=3) abolished antimycin A-evoked activation ($p<0.05$)(Fig 7). Antimycin A evoked action potential discharge from all 10 AITC-sensitive TRPV1$^{-/-}$ C-fibers, which was not significantly different to wild-type fibers ($p>0.05$)(Fig 7). Whereas, antimycin A failed to activate AITC-insensitive TRPV1$^{-/-}$ C-fibers (n=7, $p<0.05$)(Fig 7). Furthermore, pretreatment of AITC-sensitive TRPV1$^{-/-}$ C-fibers with the TRPA1 inhibitor A967079 (30 μM) reduced antimycin A-evoked activation ($p<0.05$, Fig 7), with 8 out of 11 C-fibers responding. Antimycin A also evoked no response from AITC-insensitive TRPV1$^{-/-}$ C-fibers pretreated with A967079 (n=4)(Fig 7). These data demonstrate that both TRPA1 and TRPV1 mediate antimycin A-induced activation of bronchopulmonary C-fibers. Lastly, we investigated the role of oxidative stress in the TRPA1-mediated activation of bronchopulmonary C-fibers by antimycin A. Pretreatment of AITC-sensitive TRPV1$^{-/-}$ C-fibers with MnTMPyP (50 μM) and tempol (100 μM) reduced the antimycin A-evoked activation ($p<0.05$)(Fig 7). Although all 8 C-fibers responded, this decreased activation suggests that TRPA1-mediated activation was sensitive to the antioxidant combination.

3. Discussion

The purpose of this study was to determine the specific contribution of TRPA1 and TRPV1 to the activation of vagal sensory nerves by mitochondrial dysfunction caused by antimycin A, and the role of ROS in these separate pathways. These mechanisms were studied in dissociated vagal sensory neurons, in TRP-expressing HEK293 cells and at the peripheral nerve terminals of vagal bronchopulmonary C-fibers. Antimycin A is an inhibitor of mETC complex III (Stowe and Camara, 2009), and it causes acute mitochondrial ROS production and mitochondrial depolarization in both nociceptive and non-nociceptive vagal sensory neurons (Stanford and Taylor-Clark, 2018; Turrens et al., 1985).

TRPV1 is a well-established marker of nociceptive sensory nerves in mammals (Caterina et al., 1997; Caterina et al., 2000; Montell, 2005) as capsaicin (TRPV1 agonist) evokes pain and/or defensive reflexes from somatosensory and visceral organs; and TRPV1 is expressed on most unmyelinated vagal C-fibers (Ho et al., 2001; Undem et al., 2004), although ‘fast’-conducting C-fibers within the mouse bronchopulmonary airways lack TRPV1 and capsaicin-sensitivity (Kollarik et al., 2003). TRPA1 is expressed in a subset of nociceptive sensory neurons, with a substantial overlap with TRPV1 expression (Nassenstein et al., 2008; Wang et al., 2017).

TRPA1 is activated by electrophiles such as AITC, lipid products of peroxidation and ROS, as well as by non-electrophilic compounds such as thymol (Andersson et al., 2008; Jordt et al., 2004; Sawada et al., 2008; Taylor-Clark et al., 2008a). AITC and ROS (e.g. H_2O_2) evoke pain and/or defensive reflexes in a largely TRPA1-dependent manner (Bautista et al., 2006; Bessac et al., 2008). Here, we used a TRPV1 reporter mouse (TRPV1$^{Cre/+}$/ROSA26-tdTomato$^{fl/+}$), which showed a strong correlation between tdTomato expression and capsaicin sensitivity in the vagal ganglia. However, a small subpopulation of tdTomato-expressing neurons failed to respond to capsaicin, likely due to a lack of TRPV1 expression as had been previously reported in other sensory ganglia (Cavanaugh et al., 2011). This

sensory population may have expressed TRPV1 at some earlier developmental stage, although their function in the vagal system is not presently known. Approximately 50% of tdTomato-expressing neurons were sensitive to AITC, consistent with previous reports that TRPA1 is expressed in a subpopulation of TRPV1-expressing vagal neurons. Our data indicated approximately 15% of tdTomato-expressing neurons were activated by AITC but not capsaicin. This figure is expected to be an overestimation of $TRPA1^{+}/TRPV1^{-}$ neurons, as some capsaicin-evoked responses may have been masked by the preceding AITC-evoked responses. Very few neurons that lacked tdTomato expression responded to AITC or capsaicin. Given the uncertain function of the irritant-insensitive tdTomato-expressing neurons and the irritant-sensitive neurons that lacked tdTomato expression, we decided to include these minor groups within our broad definition of nociceptive neurons. As such only neurons that lacked both irritant sensitivity and tdTomato expression were regarded as non-nociceptive in this study.

Antimycin A evoked substantial Ca^{2+} influx in a major subpopulation of vagal nociceptive neurons (‘responding’ nociceptors), which was eliminated by the non-selective Ca^{2+} channel blockers Gd^{3+} and ruthenium red and by buffering extracellular Ca^{2+}. Antimycin A evoked only minor Ca^{2+} fluxes in non-nociceptive neurons, and again these responses were dependent on extracellular Ca^{2+}, but the underlying channel/mechanism is presently unknown. Nonnociceptive vagal neurons do not express either TRPA1 or TRPV1 (Nassenstein et al., 2008; Taylor-Clark et al., 2008a), thus these TRP channels are not required for such responses. Ca^{2+} responses in non-nociceptors were inhibited by ruthenium red alone and abolished by a combination of Gd^{3+} and ruthenium red, thus it is possible that more than one distinct mechanism contributes. Pharmacological inhibition of TRPM7, a ubiquitously expressed ROS-sensitive channel blocked by both ruthenium red and Gd^{3+} (Harding et al., 2018; Wu et al., 2010; Yoshida et al., 2006), had no effect on antimycin A-evoked responses in non-nociceptive neurons, indicating that TRPM7 was not involved. Although the functional outcome of the Ca^{2+} influx in non-nociceptors was not investigated here, antimycin A fails to evoke action potential discharge from non-nociceptive sensory afferents innervating the bronchopulmonary airways (Nesuashvili et al., 2013) and as shown in the present study simultaneous inhibition/knockout of TRPA1 and TRPV1 abolished antimycin A activation of nociceptive bronchopulmonary C-fibers (see below).

We have previously shown that antimycin A activates a subset of vagal nociceptors and these responses are reduced by inhibition or knockout of either TRPA1 or TRPV1 (Nesuashvili et al., 2013). In those studies nociceptors were defined by irritant (AITC and capsaicin) sensitivity (Nesuashvili et al., 2013; Stanford and Taylor-Clark, 2018). This approach has limitations when used in conjunction with genetic and pharmacological strategies that limit irritant sensitivity. In the case of TRPA1 interventions characterization of nociceptor status is not substantially modified because nearly all nociceptors express the capsaicin-sensitive TRPV1 and the TRPA1 inhibitor is readily reversible. For TRPV1 interventions, however, the characterization of nociceptor status is significantly impaired – the 30% of nociceptors that do not express TRPA1 are counted as non-nociceptors with $TRPV1^{-/-}$ neurons or I-RTX (which is irreversible under current protocols). Here we have used an independent marker of nociceptive status (tdTomato expression). In addition to the analysis of individual neuronal Ca^{2+} responses to antimycin and the TRP agonists, we have assessed antimycin A-

evoked populational responses in three unbiased measurements: mean Ca^{2+} response of all neurons, % of neurons responding, and mean Ca^{2+} response of responding neurons.

Surprisingly antimycin A-evoked Ca^{2+} responses in individual vagal neurons correlated with capsaicin sensitivity (TRPV1) compared to AITC sensitivity (TRPA1). Simultaneous inhibition/knockout of both TRP channels reduced the Ca^{2+} response of the total vagal neuron population to background levels and, as such, eliminated the % of neurons responding. Thus, our data indicate that TRPA1 and TRPV1 are required for vagal nociceptive responses, but their contribution is distinct: inhibition or knockout of TRPV1 produced a substantial reduction in both the Ca^{2+} response of the total vagal neuron population and the % of neurons responding, whereas inhibition of TRPA1 only reduced the Ca^{2+} response of the total vagal neuron population without having a significant effect on the % of neurons responding. The antimycin A-evoked Ca^{2+} response of the total vagal neuron population was decreased in TRPA1 knockout neurons, but this did not reach significance. It is plausible that the effect of the TRPA1 inhibitor A967079 was an off-target effect, but this compound has >2000-fold affinity for TRPA1 over other TRPs (Chen et al., 2011). Alternatively, undetermined compensatory changes in gene expression in the TRPA1 knockout could have affected the antimycin A-evoked responses. Interestingly, both inhibition and knockout of TRPA1 reduced the Ca^{2+} response of 'responding' neurons, whereas both inhibition and knockout of TRPV1 had no effect on this parameter. Clearly, inhibition/knockout of TRPV1 reduced the antimycin A-evoked Ca^{2+} responses in ~25% of vagal neurons down to levels indistinguishable from non-nociceptor responses. Thus, the apparent lack of effect of TRPV1 inhibition/knockout on the Ca^{2+} response of 'responding' neurons is due to a limited role of TRPV1 in the Ca^{2+} responses of those neurons with the greatest responses. Indeed, TRPV1 was shown to predominate in the responses of the general 'responder' population, but TRPA1 was shown to be critical to the greatest neuronal responses. It is important to note that virtually all the nociceptive population with the greatest antimycin A-evoked responses (mediated by TRPA1) also expressed TRPV1.

Analysis of TRP channel contribution to antimycin A-evoked action potential discharge from bronchopulmonary C-fiber benefits from the use of conduction velocity as an independent marker of nociceptive status. In the mouse lung, nearly all sensory fibers conducting slower than 0.7m/s are capsaicin-sensitive and are considered nociceptive (Kollarik et al., 2003). Here, we analyzed antimycin A-evoked responses in this slow C-fiber population. We found that antimycin A evoked more action potentials from AITC-sensitive C-fibers compared to AITC-insensitive C-fibers, consistent with previous studies (Nesuashvili et al., 2013). Antimycin A-evoked responses were reduced in $TRPA1^{-/-}$ C-fibers, confirming the role of TRPA1. Addition of the TRPV1 inhibitor I-RTX to TRPA1−/− abolished the response, thus indicating that the residual antimycin A-evoked responses in AITC-insensitive C-fibers and $TRPA1^{-/-}$ C-fibers were mediated only by TRPV1. Interestingly, antimycin A-evoked responses in AITC-sensitive $TRPV1^{-/-}$ C-fibers were no different to AITC-sensitive wild-type C-fibers, suggesting that compensation between TRP channel functionality may take place. Antimycin A activated all AITC-sensitive C-fibers and 50% of AITC-insensitive C-fibers. This suggests that the functional link between mitochondria and TRP channels (in particular TRPA1) is more consistent at the peripheral sensory terminal than within the soma of dissociated neurons.

TRPA1 is activated by low concentrations of ROS, such as superoxide and H_2O_2, and other electrophilic compounds produced during oxidative and nitrative stress, such as 4-hydroxynonenal, 9-nitrooleate, prostaglandin J2 and acrolein (Andersson et al., 2008; Bautista et al., 2006; Sawada et al., 2008; Taylor-Clark et al., 2008a; Taylor-Clark et al., 2008b; Taylor-Clark et al., 2009). Point mutation studies have shown that electrophiles activate TRPA1 via the covalent modification of specific cysteine residues on the intracellular N-terminus (Bahia et al., 2016; Hinman et al., 2006; Macpherson et al., 2007). However, the link between TRPV1 activation, ROS and oxidative stress is far less definitive: studies have reported that H_2O_2 does not activate TRPV1 in mouse sensory neurons at physiological concentrations (Andersson et al., 2008), although millimolar H_2O_2 can sensitize TRPV1 (Chuang and Lin, 2009) and some electrophilic carbonyl compounds (e.g. 4-oxononenal and allicin) can activate TRPV1 at high concentrations (Salazar et al., 2008; Taylor-Clark et al., 2008a). Indeed, TRPV1 is activated by reducing agents (Vyklicky et al., 2002). Here, we found that H_2O_2, in addition to activating hTRPA1 as expected, activated a subset of hTRPV1-expressing HEK293. Whereas the TRPA1 activation was consistent and normally distributed, the TRPV1 responses were either negligible or on average greater than the TRPA1 responses. The molecular mechanism of TRPV1 activation by H_2O_2 is presently unclear, although Cys157 on TRPV1 mediates activation by other electrophilic compounds (Salazar et al., 2008). The cause of the inconsistent activation of TRPV1 by H_2O_2 is also unknown, but it suggests the activation is indirect, requiring other factors. Consistent with our previous data (Nesuashvili et al., 2013), antimycin A activated both TRPA1- and TRPV1-expressing HEK293. Histograms of the magnitude of Ca^{2+} fluxes showed that antimycin A-evoked responses cannot be described by a single gaussian distribution, rather there are 2 major groupings: strong responders and weak responders. The weak responders in the hTRPA1- and hTRPV1-expressing HEK293 had only partial overlap with the non-transfected HEK293 cells, indicating that some proportion of the weak responses were specifically mediated by the TRP channels. As such, mitochondrial signaling to TRP channels in HEK293, as in neurons, is not linearly linked – i.e. it is facilitated by other unknown factors.

We have previously shown that a combination of the ROS-scavengers MnTMPyP and tempol reduced antimycin A-induced activation of hTRPA1-HEK293 cells by ~75%, although within minutes full TRPA1 activation was evoked by antimycin A (Nesuashvili et al., 2013). Here, antimycin A-evoked activation of TRPA1-expressing HEK293 was inhibited by the reducing agent DTT by ~33%. TRPA1 is a polymodal channel that can be activated by multiple redox and non-redox pathways (Bautista et al., 2006; Jordt et al., 2004; Wu et al., 2010), thus it is plausible that antimycin A activates TRPA1 via ROS-dependent and ROS-independent mechanisms. We addressed this hypothesis using a ROS-insensitive mutant of hTRPA1 (K620A (Bahia et al., 2016)). The K620A TRPA1 mutant was completely insensitive to antimycin A, confirming the unique contribution of redox-mediated activation. The lack of effectiveness of antioxidants in reducing antimycin A-evoked TRPA1 activation is likely due to the high reactivity of cysteines involved in TRPA1 electrophilic binding (Bahia et al., 2016). Despite the observation that H_2O_2 could activate TRPV1, antimycin A-evoked activation of TRPV1-expressing HEK293 was unaffected by

DTT. Thus, in this heterologous system antimycin A activated TRPA1 in a ROS-dependent manner and TRPV1 in a ROS-independent manner.

We addressed the role of ROS in antimycin A-evoked activation of vagal nociceptors in the soma of dissociated neurons and at the peripheral terminals of vagal bronchopulmonary C-fibers. Antioxidants reduced antimycin A-induced Ca^{2+} responses in TRPV1$^{-/-}$ neurons, but they had no effect on TRPA1$^{-/-}$ neuronal responses. Furthermore, the antioxidants reduced antimycin A-evoked action potential discharge from AITC-sensitive TRPV1$^{-/-}$ bronchopulmonary C-fibers. Thus, our neuronal data are similar to the HEK293 data: mitochondrial signaling to TRPA1 is ROS-dependent but signaling to TRPV1 is ROS-independent. This is consistent with the correlation of calcium responses and mitochondrial ROS production in antimycin A-treated dissociated vagal neurons: there was a positive correlation in wild-type and TRPV1$^{-/-}$ neurons, but no correlation in TRPA1$^{-/-}$ neurons (Stanford and Taylor-Clark, 2018). Nevertheless, the correlation in wild-type neurons is not particularly strong as some nociceptors with substantial mitochondrial ROS production had little or no Ca^{2+} response to antimycin A, and the mean ROS production was no different between ‘responding’ and ‘non-responding’ nociceptive populations (Stanford and Taylor-Clark, 2018). Here, we have found that the % of neurons responding with TRPV1 inhibition/knockout (i.e. conditions when only TRPA1 was available) was ~12%. Given that TRPA1 is expressed in ~50% of vagal nociceptors, this suggests that ROS signaling caused the activation of only a quarter of TRPA1-expressing nociceptors in TRPV1 inhibition/knockout conditions, thus indicating that other unknown factors are required to permit mitochondrial ROS-mediated activation of neuronal TRPA1.

The mechanism linking mitochondrial signaling with TRPV1 activation is presently unknown. Antimycin A-evoked hTRPV1 activation in HEK293 cells was eliminated in whole cell patch clamp studies but preserved in gramicidin-perforated patch clamp (Nesuashvili et al., 2013). This is consistent with an indirect activation of TRPV1 by antimycin, likely involving soluble factors. In addition to ROS production, antimycin A causes mitochondrial depolarization. We have previously reported that antimycin A-evoked Ca^{2+} responses in wild-type neurons fails to correlate with mitochondrial depolarization, largely due to the fact that 97% of neurons were depolarized in these studies (Stanford and Taylor-Clark, 2018). Mitochondrial dysfunction also impacts multiple signaling processes such as cytosolic calcium (Gover et al., 2007; Gunter et al., 2004), phospholipase A2 (Rauckhorst et al., 2015), phospholipase C (Knox et al., 2004), protein kinase A (Hongpaisan et al., 2004), protein kinase C (Hadley et al., 2014; Rathore et al., 2006), and nuclear factor of activated T-cells (NFAT) (Kim and Usachev, 2009). TRPV1 is a polymodal ion channel whose activation is regulated by multiple lipid signaling molecules including phosphatidylinositol 4,5-bisphosphate and 15-(S)-hydroperoxyeicosatetraenoic acids (Hardie, 2007; Hwang et al., 2000; Ufret-Vincenty et al., 2011). Further studies are required to elucidate the ROS-independent mechanism of mitochondrial dysfunction-induced TRPV1 activation.

In conclusion, we have shown for the first time that TRPV1 rather than TRPA1 contributes to the majority of the Ca^{2+} responses to antimycin A in vagal nociceptive neurons, and that antimycin A activates nociceptors via ROS-dependent (TRPA1) and ROS-independent

(TRPV1) mechanisms in both the cell soma and the peripheral terminals of bronchopulmonary C-fibers. Thus both ROS-independent and ROS-dependent nociceptive mechanisms will likely contribute to excessive nociceptive signaling in inflammatory states where mitochondrial dysfunction occurs.

4. Experimental Procedures

4.1 Mouse Models

TRPV1$^{Cre/Cre}$ (Trpv1tm1(cre)Bbm, 017769, Jackson Laboratory) were mated with ROSA26-tdTomato$^{fl/fl}$ (B6.Cg-Gt(ROSA)26Sortm9(CAG-tdTomato)Hze/J, 007909, Jackson Laboratory) to yield TRPV1$^{Cre/+}$/ROSA26-tdTomato$^{fl/+}$ mice. Female TRPV1$^{-/-}$ mice were mated with male TRPV1$^{-/-}$ mice (B6.129X1-Trpv1tm1Jul/J, 003770, Jackson Laboratory). Female TRPA1$^{-/-}$ mice were mated with male TRPA1$^{+/-}$ mice (B6;129P-Trpa1tm1Kykw/J, 006401, Jackson Laboratory). Genotype of the offspring was confirmed using polymerase chain reaction. Wild type C57BL/6J mice were purchased from Jackson Laboratory (000664). All experiments were performed with approval from the University of South Florida Institutional Animal Care and Use Committee (AAALAC #000434).

4.2 Vagal ganglia dissociation

Male 6–12-week-old TRPV1$^{Cre/+}$/ROSA26-tdTomato$^{fl/+}$, TRPV1$^{-/-}$ and TRPA1$^{-/-}$ mice were euthanized by CO_2 asphyxiation followed by exsanguination. As previously described (Stanford and Taylor-Clark, 2018), vagal ganglia were isolated in Ca^{2+}-free, Mg^{2+}-free Hank's buffered saline solution HBSS, then incubated in HBSS containing collagenase (2mg/ml) and dispase (2mg/ml), then mechanically dissociated with fire-polished pipettes. Individual neurons were washed with L-15 media supplemented with 10% fetal bovine serum, 100 U/ml penicillin and 100 μg/ml streptomycin then plated onto poly-D-lysine and laminin coated coverslips. Neurons were incubated at 37°C in antibiotic-free L-15 media supplemented with 10% fetal bovine serum and used within 24 hours.

4.3 HEK293 culture

Full-length human TRPA1 (hTRPA1) and hTRPV1 were subcloned into pcDNA3.1 V5-His-TOPO® (Life Technologies; Grand Island, NY) using primers (Biosynthesis, Lewisville, TX) containing restriction sites allowing ligation into the vector. The point mutation to create hTRPA1-K620A mutant was made by PCR, as described previously (Bahia et al., 2016). TRP channels were expressed in HEK293 cells (cultured in Dulbecco's modified Eagles' medium supplemented with 10% FBS, 100 U/ml penicillin and 100 μg/ml streptomycin) using Lipofectamine® 2000.

4.4 Live cell Ca^{2+} imaging

Cells were incubated with 4μM FURA-2AM for 30–60 minutes at 37°C. Coverslips were loaded into a chamber on an inverted microscope and perfused with heated (33–34°C) HEPES buffer (154mM NaCl, 1.2mM KCl, 1.2mM $MgCl_2$, 2.5mM $CaCl_2$, 5.6mM D-Glucose). Slides equilibrated for 10 minutes prior to the start of the experiment and, if using the TRPV1$^{Cre/+}$/ROSA26-tdTomato$^{fl/+}$ neurons, an image was taken to visualize tdTomato fluorescence (535nm excitation, 610nm emission). Changes in $[Ca^{2+}]_i$ was monitored using

sequential excitation at 340nm and 380nm (510nm emission) with images taken every 6 seconds using a CoolSnap HQ2 camera (Photometrics) and evaluated ratiometrically using the 340/380 ratio.

All drugs were diluted in HEPES buffer. Following 10 μM antimycin A (3 min application), TRPA1 and TRPV1 expression was tested by treatment with 100 μM AITC (TRPA1 agonist) and 1 μM capsaicin (TRPV1 agonist). The maximal Ca^{2+} response was evaluated using 5 μM ionomycin. For neuronal studies, the neurons were further characterized by response to KCl (75mM) prior to ionomycin. In some cases, the expression of hTRPA1 constructs in HEK293 was determined using thymol (200 μM). In specific experiments TRPA1 was inhibited by 5 min pretreatment with A967079 (5 μM) (McGaraughty et al., 2010), and TRPV1 was inhibited by 1 min pretreatment with iodoresiniferatoxin (I-RTX, 500 nM) (Wahl et al., 2001). Both drugs were washed out 1 min following antimycin A washout, but previous studies show that I-RTX's inhibition of TRPV1 under these conditions is not reversible (Taylor-Clark et al., 2008a). ROS were scavenged using a combination of MnTMPyP (Day et al., 1997) and tempol (Krishna et al., 1996): neurons were first incubated with tempol (1mM) for 90 mins, then neurons were perfused with HEPES buffer containing MnTMPyP (50 μM) and tempol (100 μM) for 15 mins prior to antimycin A treatment.

4.5 Imaging analysis

Image analysis was performed by using Nikon Elements (Nikon, Melville, NY) by drawing individual regions of interest (ROI) that around the intracellular region for each cell and tracked over time. ROI's with an unstable, high, or noisy baseline were eliminated from analysis. Neurons which failed to exhibit an increase in $[Ca^{2+}]_i$ to either AITC, capsaicin or KCl challenges (> 30% the ionomycin maximal response) were eliminated. HEK293 cells failing to exhibit an increased $[Ca^{2+}]_i$ in response to AITC/thymol (TRPA1 transfected) or capsaicin (TRPV1 transfected) were omitted. Relative changes in $[Ca^{2+}]_i$ were determined ratiometrically using Fura-2 fluorescence: 340/380 ratio (R). This negates the impact of cell to cell variations in FURA-2AM loading.

In the time series analyses, changes in the 340/380 ratio ($\Delta R = R_1 - R_0$) are presented, where R0 is the average 340/380 ratio prior to antimycin treatment. In the bar graphs, scatterplots and statistical analyses, the response to antimycin A, AITC or capsaicin was determined using the maximal Δ340/380 ($\Delta R_{max} = R_{max} - R_0$) for each neuron. Response to either AITC (TRPA1) or capsaicin (TRPV1) allows for functional characterization of nociceptive status (Stanford and Taylor-Clark, 2018). An individual neuron was considered to be sensitive to a TRP agonist if $R_{TRP} > (R_{bl} + 2*SD_{bl})$; where R_{TRP} is the average 340/380 ratio during AITC/capsaicin treatment, R_{bl} is the average 340/380 ratio prior to TRP agonist treatment, and SD_{bl} is the standard deviation of R_{bl}. In many experiments vagal neurons from $TRPV1^{Cre/+}$/ROSA26-$tdTomato^{fl/+}$ mice were used. These neurons express tdTomato in TRPV1-lineage cells. Nociceptive status was characterized by sensitivity to TRP agonists or the expression of tdTomato. As before (Stanford and Taylor-Clark, 2018), a nociceptive neuron was defined as 'responding' to antimycin A during the 3 min application if the $[Ca^{2+}]_i$ ΔR_{max} was greater than 3 * SD of the ΔR_{max} of non-nociceptors: $\Delta R_{max(noci)} > \Delta R_{max(nonnoci)} + 3 * SD_{(nonnoci)}$ where $\Delta R_{max(noci)}$ is the maximal response to antimycin A

in an individual nociceptor, $\Delta R_{max(nonnoci)}$ is the average maximal response in non-nociceptors, and $SD_{(nonnoci)}$ is the standard deviation of $\Delta R_{max(nonnoci)}$. Given that antimycin A activates only a subset of neurons, we have evaluated antimycin A's effects using three different populational parameters: the mean $[Ca^{2+}]_i$ response of all vagal sensory neurons, the % of neurons responding, and mean $[Ca^{2+}]_i$ response of 'responding' neurons. In addition, histograms were derived for the ΔR_{max} for antimycin A responses in each neuron (0.04 per bin). Neurons were grouped by classification: non-nociceptor, 'non-responding' nociceptor and 'responding' nociceptor. In the case of $TRPA1^{-/-}$ neurons pretreated with I-RTX nociceptor status is undefinable and neurons were allocated to 'responding' neuron and 'non-responding' neuron.

4.6 Bronchopulmonary C-fiber extracellular recordings

Male C57BL/6J, $TRPA1^{-/-}$ and $TRPV1^{-/-}$ mice (6–10 weeks) were killed by CO_2 asphyxiation followed by exsanguination. The innervated isolated lung preparation was prepared as previously described (Nassenstein et al., 2008; Nesuashvili et al., 2013). Briefly, the airways and lungs with their intact extrinsic innervation (vagus nerve including vagal ganglia) were taken and placed in a dissecting dish containing Krebs bicarbonate buffer solution composed of (mM): 118 NaCl, 5.4 KCl, 1.0 NaH_2PO_4, 1.2 $MgSO_4$, 1.9 $CaCl_2$, 25.0 $NaHCO_3$ and 11.1 D-glucose, and equilibrated with 95% O_2 and 5% CO_2 (pH 7.3–7.4) and containing 3 μM indomethacin. Connective tissue was trimmed away leaving the trachea and lungs with their intact nerves. The airways were then pinned to the larger compartment of a custom-built two-compartment recording chamber that was lined with silicone elastomer (Sylgard). A vagal ganglion was pulled into the adjacent compartment of the chamber through a small hole and pinned. Both compartments were separately superfused with Krebs bicarbonate buffer (37°C). A sharp glass electrode was pulled by a Flaming Brown micropipette puller (P-87; Sutter Instruments, Novato, CA, USA) and filled with 3 M NaCl solution. The electrode was inserted and placed near the cell bodies of vagal ganglion. The recorded action potentials were amplified (Microelectrode AC amplifier 1800; A-M Systems, Everett, WA, USA), filtered (0.3 kHz of low cut-off and 1 kHz of high cut-off), and monitored on an oscilloscope (TDS1002B; Tektronix, Beaverton, OR, USA). The scaled output from the amplifier was captured and analyzed by a Macintosh computer using NerveOfIt software (Phocis, Baltimore, MD, USA). To measure conduction velocity, an electrical stimulation (S44; Grass Instruments, Quincy, MA, USA) was applied to the center of the receptive field. The conduction velocity of the individual bronchopulmonary afferent was calculated by dividing the distance along the nerve pathway by the time delay between the shock artifact and the action potential evoked by electrical stimulation. Drugs were intratracheally applied as a 1 ml bolus over 10 s. The viability of a given bronchopulmonary C-fiber terminal was determined by action potential discharge to mechanical stimuli (von Frey fibers). C-fibers were characterized for their expression of TRPA1 and TRPV1 channels by their response to AITC (30 μM) and the capsaicin (1 μM), respectively. Due to a lack of TRPV1 channels in bronchopulmonary C-fibers from $TRPV1^{-/-}$ mice, 'nociceptive' status was assessed solely by conduction velocity and the response to TRPA1 agonists (Kollarik et al., 2003; Nassenstein et al., 2008). Only one antimycin A (20 μM) treatment was used per preparation. Due to potential heterologous desensitization, capsaicin was only given at the end of each experiment. All excitatory chemical treatments were separated by at

least 15 mins. TRPA1 was inhibited with A967079 (30 μM). TRPV1 was inhibited with I-RTX (1 μM). ROS scavenging was achieved with MnTMPyP (50 μM) and tempol (100 μM). All TRP and ROS inhibitors were perfused for 10 minutes preceding and subsequent to antimycin A application. Action potential discharge was quantified off-line and recorded in 1 s bins. A response was considered positive if the number of action potentials in any 1 s bin was twice the average background response. The background activity was usually either absent or less than 2 Hz. Antimycin A-evoked responses were quantified as the total number of action potentials recorded in 600s after application.

4.7 Statistical analyses

Data and statistical analyses were performed using Microsoft Excel, R studio and GraphPad Prism 7. To determine statistical differences in $[Ca^{2+}]_i$ in specific neuronal populations we performed two-way ANOVAs followed by post hoc comparison using the Bonferroni correction. To evaluate the correlation between antimycin-evoked Ca^{2+} responses and TRP agonist Ca^{2+} responses, we performed a one-tailed Pearson correlation. A chi square test for homogeneity was used to evaluate the percentage of 'responding' neurons under each condition. To determine statistical differences in total action potential discharge to antimycin A or conduction velocity in specific neuronal populations we performed two-way ANOVAs followed by post hoc comparison using the Bonferroni correction. A p value of 0.05 was taken as the threshold for significance.

4.8 Chemicals

Fura-2AM was purchased from TEFLabs (Austin, TX). DMSO were purchased from Thermo Fisher Scientific (Waltham, MA). Ionomycin was purchased from LKT Laboratories (St. Paul, MN). A967079 and I-RTX were purchased from Tocris (Ellisville, MO). All other reagents were purchased from Sigma-Aldrich (St. Louis, MO).

Acknowledgements

The plasmid containing full-length hTRPA1 was a kind gift of David Julius (University of California, San Francisco). The plasmid containing full-length hTRPV1 was obtained from the Center for Personalized Diagnostics via the DNASU plasmid repository (HsCD00731917). This work was supported by the National Institutes of Health (R01HL119802).

Abbreviations

AITC	Allyl isothiocyanate
I-RTX	iodoresiniferatoxin
mETC	mitochondrial electron transport chain
ROS	reactive oxygen species
TRP	Transient receptor potential
TRPA1	Transient receptor potential ankyrin 1
TRPV1	Transient receptor potential vanilloid 1

References

Andersson DA, et al., 2008 Transient receptor potential A1 is a sensory receptor for multiple products of oxidative stress. J Neurosci. 28, 2485–94. [PubMed: 18322093]

Bahia PK, et al., 2016 The exceptionally high reactivity of Cys 621 is critical for electrophilic activation of the sensory nerve ion channel TRPA1. J Gen Physiol. 147, 451–65. [PubMed: 27241698]

Bautista DM, et al., 2006 TRPA1 Mediates the Inflammatory Actions of Environmental Irritants and Proalgesic Agents. Cell. 124, 1269–82. [PubMed: 16564016]

Bessac BF, et al., 2008 TRPA1 is a major oxidant sensor in murine airway sensory neurons. J Clin Invest. 118, 1899–910. [PubMed: 18398506]

Brunelle JK, et al., 2005 Oxygen sensing requires mitochondrial ROS but not oxidative phosphorylation. Cell Metab. 1, 409–14. [PubMed: 16054090]

Caterina MJ, et al., 1997 The capsaicin receptor: a heat-activated ion channel in the pain pathway. Nature. 389, 816–24. [PubMed: 9349813]

Caterina MJ, et al., 2000 Impaired nociception and pain sensation in mice lacking the capsaicin receptor. Science. 288, 306–13. [PubMed: 10764638]

Cavanaugh DJ, et al., 2011 Trpv1 reporter mice reveal highly restricted brain distribution and functional expression in arteriolar smooth muscle cells. J Neurosci. 31, 5067–77. [PubMed: 21451044]

Chen J, et al., 2011 Selective blockade of TRPA1 channel attenuates pathological pain without altering noxious cold sensation or body temperature regulation. Pain. 152, 1165–72. [PubMed: 21402443]

Chuang HH, Lin S, 2009 Oxidative challenges sensitize the capsaicin receptor by covalent cysteine modification. Proc Natl Acad Sci U S A. 106, 20097–102. [PubMed: 19897733]

Chubanov V, et al., 2012 Natural and synthetic modulators of SK (K(ca)2) potassium channels inhibit magnesium-dependent activity of the kinase-coupled cation channel TRPM7. Br J Pharmacol. 166, 1357–76. [PubMed: 22242975]

Corda S, et al., 2001 Rapid reactive oxygen species production by mitochondria in endothelial cells exposed to tumor necrosis factor-alpha is mediated by ceramide. Am J Respir Cell Mol Biol. 24, 762–8. [PubMed: 11415943]

Day BJ, Fridovich I, Crapo JD, 1997 Manganic porphyrins possess catalase activity and protect endothelial cells against hydrogen peroxide-mediated injury. Arch Biochem Biophys. 347, 256–62. [PubMed: 9367533]

Gover TD, et al., 2007 Calcium regulation in individual peripheral sensory nerve terminals of the rat. J Physiol. 578, 481–90. [PubMed: 17095566]

Gunter TE, et al., 2004 Calcium and mitochondria. FEBS Lett. 567, 96–102. [PubMed: 15165900]

Hadley SH, Bahia PK, Taylor-Clark TE, 2014 Sensory nerve terminal mitochondrial dysfunction induces hyperexcitability in airway nociceptors via protein kinase C. Mol Pharmacol. 85, 839–48. [PubMed: 24642367]

Hardie RC, 2007 TRP channels and lipids: from Drosophila to mammalian physiology. J Physiol. 578, 9–24. [PubMed: 16990401]

Harding SD, et al., 2018 The IUPHAR/BPS Guide to PHARMACOLOGY in 2018: updates and expansion to encompass the new guide to IMMUNOPHARMACOLOGY. Nucleic Acids Res. 46, D1091–d1106. [PubMed: 29149325]

Hinman A, et al., 2006 TRP channel activation by reversible covalent modification. Proc Natl Acad Sci U S A. 103, 19564–8. [PubMed: 17164327]

Ho CY, et al., 2001 Sensitivity of vagal afferent endings to chemical irritants in the rat lung. Respir Physiol. 127, 113–24. [PubMed: 11504584]

Hongpaisan J, Winters CA, Andrews SB, 2004 Strong calcium entry activates mitochondrial superoxide generation, upregulating kinase signaling in hippocampal neurons. J Neurosci. 24, 10878–87. [PubMed: 15574738]

Hung KS, et al., 1973 Ultrastructure of nerves and associated cells in bronchiolar epithelium of the mouse lung. J Ultrastruct Res. 43, 426–37. [PubMed: 4578329]

Hwang SW, et al., 2000 Direct activation of capsaicin receptors by products of lipoxygenases: endogenous capsaicin-like substances. Proc Natl Acad Sci U S A. 97, 6155–60. [PubMed: 10823958]

Jones RC 3rd, Xu L, Gebhart GF, 2005 The mechanosensitivity of mouse colon afferent fibers and their sensitization by inflammatory mediators require transient receptor potential vanilloid 1 and acid-sensing ion channel 3. J Neurosci. 25, 10981–9. [PubMed: 16306411]

Jordt SE, et al., 2004 Mustard oils and cannabinoids excite sensory nerve fibres through the TRP channel ANKTM1. Nature. 427, 260–5. [PubMed: 14712238]

Kim MS, Usachev YM, 2009 Mitochondrial Ca2+ cycling facilitates activation of the transcription factor NFAT in sensory neurons. J Neurosci. 29, 12101–14. [PubMed: 19793968]

Knox CD, et al., 2004 Novel role of phospholipase C-delta1: regulation of liver mitochondrial Ca2+ uptake. Am J Physiol Gastrointest Liver Physiol. 287, G533–40. [PubMed: 15107298]

Kollarik M, et al., 2003 Capsaicin-sensitive and -insensitive vagal bronchopulmonary C-fibres in the mouse. J Physiol. 551, 869–79. [PubMed: 12909686]

Krishna MC, et al., 1996 Do nitroxide antioxidants act as scavengers of O2-. or as SOD mimics? J Biol Chem. 271, 26026–31. [PubMed: 8824242]

Macpherson LJ, et al., 2007 Noxious compounds activate TRPA1 ion channels through covalent modification of cysteines. Nature. 445, 541–5. [PubMed: 17237762]

McGaraughty S, et al., 2010 TRPA1 modulation of spontaneous and mechanically evoked firing of spinal neurons in uninjured, osteoarthritic, and inflamed rats. Mol Pain. 6, 14. [PubMed: 20205719]

Michaeloudes C, et al., 2010 TGF-{beta} regulates Nox4, MnSOD and catalase expression and IL-6 release in airway smooth muscle cells. Am J Physiol Lung Cell Mol Physiol.

Mishra SK, et al., 2011 TRPV1-lineage neurons are required for thermal sensation. Embo J. 30, 582–93. [PubMed: 21139565]

Montell C, 2005 The TRP superfamily of cation channels. Sci STKE 2005, re3. [PubMed: 15728426]

Nassenstein C, et al., 2008 Expression and function of the ion channel TRPA1 in vagal afferent nerves innervating mouse lungs. J Physiol. 586, 1595–604. [PubMed: 18218683]

Nesuashvili L, et al., 2013 Sensory nerve terminal mitochondrial dysfunction activates airway sensory nerves via transient receptor potential (TRP) channels. Mol Pharmacol. 83, 1007–19. [PubMed: 23444014]

Patapoutian A, Tate S, Woolf CJ, 2009 Transient receptor potential channels: targeting pain at the source. Nat Rev Drug Discov. 8, 55–68. [PubMed: 19116627]

Pehar M, et al., 2007 Mitochondrial superoxide production and nuclear factor erythroid 2-related factor 2 activation in p75 neurotrophin receptor-induced motor neuron apoptosis. J Neurosci. 27, 7777–85. [PubMed: 17634371]

Rathore R, et al., 2006 Mitochondrial ROS-PKCepsilon signaling axis is uniquely involved in hypoxic increase in [Ca2+]i in pulmonary artery smooth muscle cells. Biochem Biophys Res Commun. 351, 784–90. [PubMed: 17087917]

Rauckhorst AJ, Pfeiffer DR, Broekemeier KM, 2015 The iPLA(2)gamma is identified as the membrane potential sensitive phospholipase in liver mitochondria. FEBS Lett. 589, 2367–71. [PubMed: 26206229]

Salazar H, et al., 2008 A single N-terminal cysteine in TRPV1 determines activation by pungent compounds from onion and garlic. Nat Neurosci. 11, 255–61. [PubMed: 18297068]

Sawada Y, et al., 2008 Activation of transient receptor potential ankyrin 1 by hydrogen peroxide. Eur J Neurosci. 27, 1131–42. [PubMed: 18364033]

Stanford KR, Taylor-Clark TE, 2018 Mitochondrial modulation-induced activation of vagal sensory neuronal subsets by antimycin A, but not CCCP or rotenone, correlates with mitochondrial superoxide production. PLoS One. 13, e0197106. [PubMed: 29734380]

Stowe DF, Camara AK, 2009 Mitochondrial reactive oxygen species production in excitable cells: modulators of mitochondrial and cell function. Antioxid Redox Signal. 11, 1373–414. [PubMed: 19187004]

Taylor-Clark TE, et al., 2008a Relative contributions of TRPA1 and TRPV1 channels in the activation of vagal bronchopulmonary C-fibres by the endogenous autacoid 4-oxononenal. J Physiol. 586, 3447–59. [PubMed: 18499726]

Taylor-Clark TE, et al., 2008b Prostaglandin-induced activation of nociceptive neurons via direct interaction with transient receptor potential A1 (TRPA1). Mol Pharmacol. 73, 274–81. [PubMed: 18000030]

Taylor-Clark TE, et al., 2009 Nitrooleic acid, an endogenous product of nitrative stress, activates nociceptive sensory nerves via the direct activation of TRPA1. Mol Pharmacol. 75, 820–9. [PubMed: 19171673]

Trankner D, et al., 2014 Population of sensory neurons essential for asthmatic hyperreactivity of inflamed airways. Proc Natl Acad Sci U S A. 111, 11515–20. [PubMed: 25049382]

Turrens JF, Alexandre A, Lehninger AL, 1985 Ubisemiquinone is the electron donor for superoxide formation by complex III of heart mitochondria. Arch Biochem Biophys. 237, 408–14. [PubMed: 2983613]

Ufret-Vincenty CA, et al., 2011 Localization of the PIP2 sensor of TRPV1 ion channels. J Biol Chem. 286, 9688–98. [PubMed: 21224382]

Undem BJ, et al., 2004 Subtypes of vagal afferent C-fibres in guinea-pig lungs. J Physiol. 556, 905–17. [PubMed: 14978204]

Usoskin D, et al., 2015 Unbiased classification of sensory neuron types by large-scale single-cell RNA sequencing. Nat Neurosci. 18, 145–53. [PubMed: 25420068]

von During M, Andres KH, 1988 Structure and functional anatomy of visceroreceptors in the mammalian respiratory system. Prog Brain Res. 74, 139–54. [PubMed: 3055045]

Vyklicky L, et al., 2002 Reducing agent dithiothreitol facilitates activity of the capsaicin receptor VR-1. Neuroscience. 111, 435–41. [PubMed: 12031340]

Wahl P, et al., 2001 Iodo-resiniferatoxin, a new potent vanilloid receptor antagonist. Mol Pharmacol. 59, 9–15. [PubMed: 11125018]

Wang J, et al., 2017 Distinct and common expression of receptors for inflammatory mediators in vagal nodose versus jugular capsaicin-sensitive/TRPV1-positive neurons detected by low input RNA sequencing. PLoS One. 12, e0185985. [PubMed: 28982197]

West AP, et al., 2011 TLR signalling augments macrophage bactericidal activity through mitochondrial ROS. Nature. 472, 476–80. [PubMed: 21525932]

Wu LJ, Sweet TB, Clapham DE, 2010 International Union of Basic and Clinical Pharmacology. LXXVI. Current progress in the mammalian TRP ion channel family. Pharmacol Rev. 62, 381–404. [PubMed: 20716668]

Yoshida T, et al., 2006 Nitric oxide activates TRP channels by cysteine S-nitrosylation. Nat Chem Biol. 2, 596–607. [PubMed: 16998480]

Highlights

- Antimycin A-induced mitochondrial dysfunction activates a subset of vagal nociceptors
- Antimycin A-evoked Ca^{2+} fluxes correlate with capsaicin (TRPV1) responses
- TRPV1 and TRPA1 contribute to distinct Ca^{2+} responses
- ROS are required for antimycin A-evoked activation of TRPA1 but not TRPV1

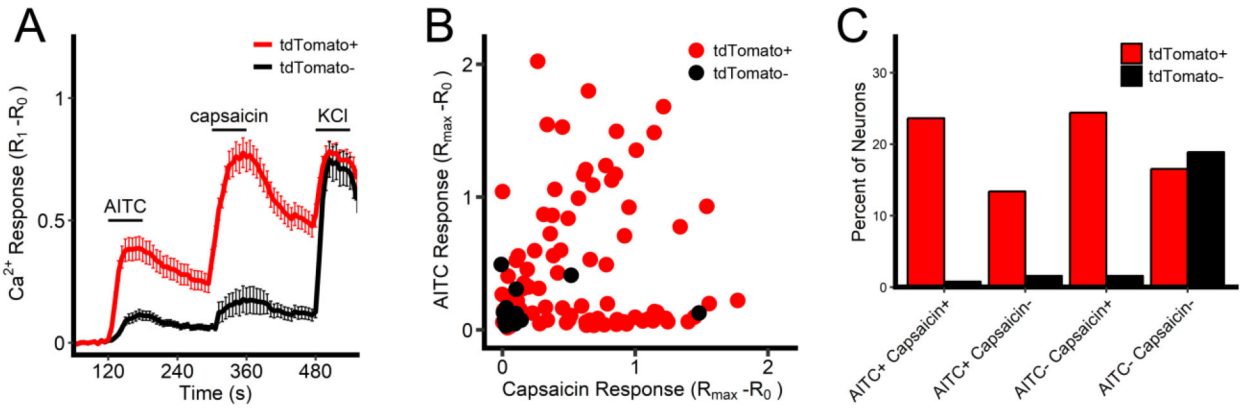

Fig 1:

Characterization of TRP channel sensitivity in vagal sensory neurons from TRPV1$^{Cre/+}$/ROSA26-tdTomato$^{fl/+}$ mice. A, Mean +/− SEM $[Ca^{2+}]_i$ responses in tdTomato-positive (red line) and tdTomato-negative (black line) neurons to AITC (100μM), capsaicin (1μM) and KCl (75mM). B, Maximal $[Ca^{2+}]_i$ response to AITC and capsaicin for each tdTomato-positive (red dot) and each tdTomato-negative (black dot) neuron. C, percentage of total neuronal population characterized by tdTomato expression and TRP agonist sensitivity.

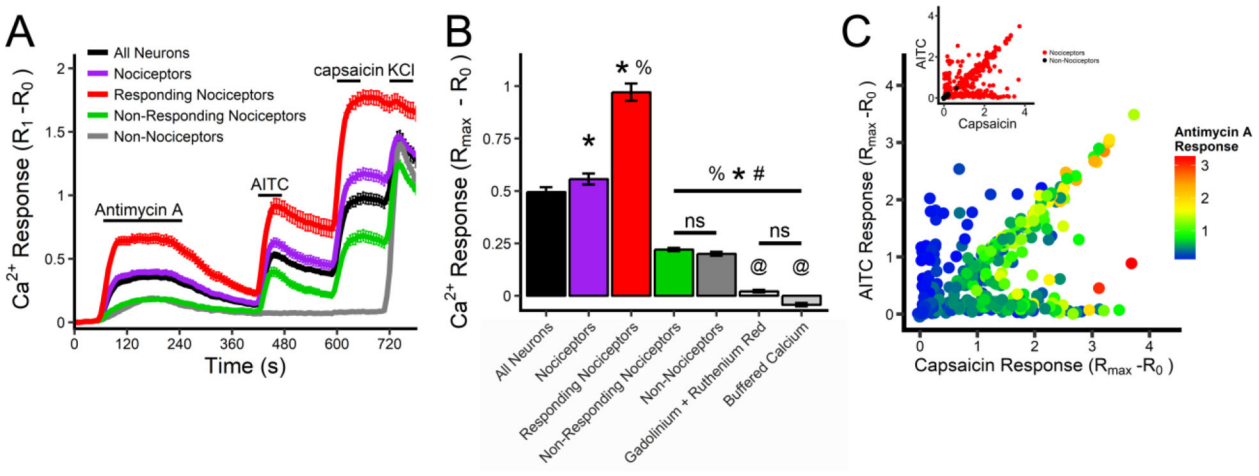

Fig 2:

Antimycin A evokes Ca2+ influx in a subset of vagal sensory neurons. A, Mean +/− SEM $[Ca^{2+}]_i$ responses in vagal neuronal subsets to antimycin A (10μM), AITC (100μM), capsaicin (1μM) and KCl (75mM). Subsets defined by their expression of tdTomato, their sensitivity to TRP channel agonists and their response to antimycin A: all neurons (black line), all nociceptors (purple line), nociceptors responding to antimycin A (red line), nociceptors insensitive to antimycin A (green line) and non-nociceptors (grey line). B, Mean maximal $[Ca^{2+}]_i$ response to antimycin A for each subset. Light grey columns represent data from all neurons in pretreated with ruthenium red (30 μM) and Gd^{3+} (300 μM), or with extracellular $[Ca^{2+}]$ buffered to 100nM. * denotes significant different from all neurons population ($p<0.05$), % denotes significant difference from all nociceptor population ($p<0.05$), # denotes significant difference from 'responding' nociceptor population ($p<0.05$), @ denotes significant difference from nonnociceptive population ($p<0.05$), ns denotes no significant difference. C, Maximal $[Ca^{2+}]_i$ response to antimycin A (rainbow color range), AITC (y axis) and capsaicin (x axis) for each neuron from the entire vagal population. Inset, maximal $[Ca^{2+}]_i$ response to AITC and capsaicin for each tdTomato-positive (red dot) and each tdTomato-negative (black dot) neuron.

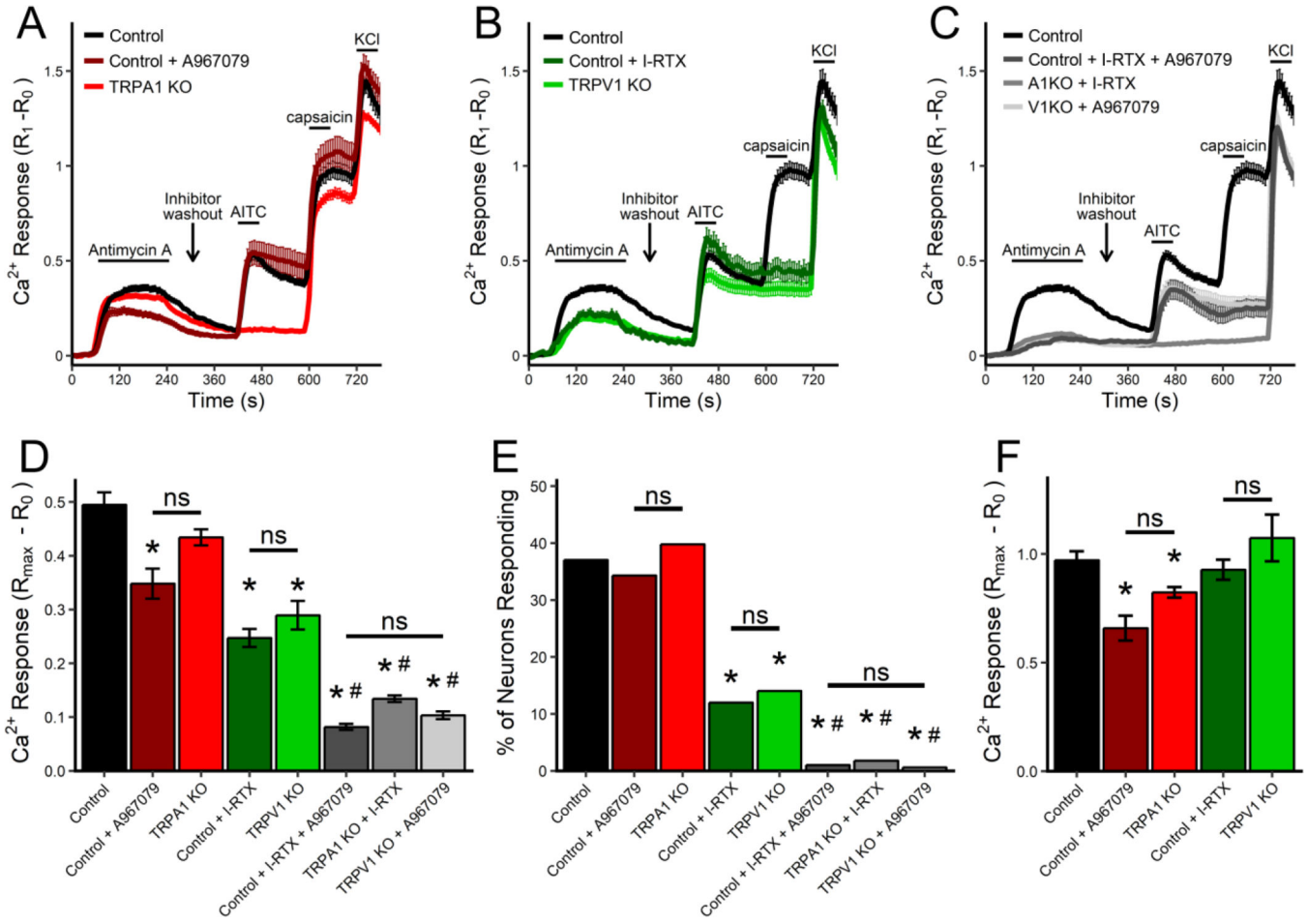

Fig 3:

Antimycin A-induced Ca2+ responses in vagal sensory neurons is mediated by TRPA1 and TRPV1. A–C, Mean +/− SEM $[Ca^{2+}]_i$ responses of the total vagal population to antimycin A (10μM), AITC (100μM), capsaicin (1μM) and KCl (75mM) from $TRPV1^{Cre/+}$/ROSA26-$tdTomato^{fl/+}$ mice (Control, black line). A, Mean +/− SEM $[Ca^{2+}]_i$ responses in control vagal neurons pretreated with A967079 (5μM, dark red line) or in vagal neurons from TRPA1−/− mice (TRPA1 KO, red line). B, Mean +/− SEM $[Ca^{2+}]_i$ responses in control vagal neurons pretreated with I-RTX (500nM, dark green line) or in vagal neurons from TRPV1−/− mice (TRPV1 KO, green line). C, Mean +/− SEM $[Ca^{2+}]_i$ responses in control vagal neurons pretreated with I-RTX and A967079 (dark grey line) or in vagal neurons from TRPA1−/− mice (A1KO) pretreated with I-RTX (grey line) or in vagal neurons from TRPV1−/− mice (V1KO) pretreated with A967079 (light grey line). D, Mean maximal $[Ca^{2+}]_i$ response to antimycin A for the total vagal population under each condition. E, percentage of total vagal population responding to antimycin A under each condition. F, Mean maximal $[Ca^{2+}]_i$ response to antimycin A of 'responding' neurons under each condition. * denotes significant difference from control neurons ($p<0.05$), # denotes significant difference from inhibition/knockout of a single TRP channel ($p<0.05$), ns denotes no significant difference.

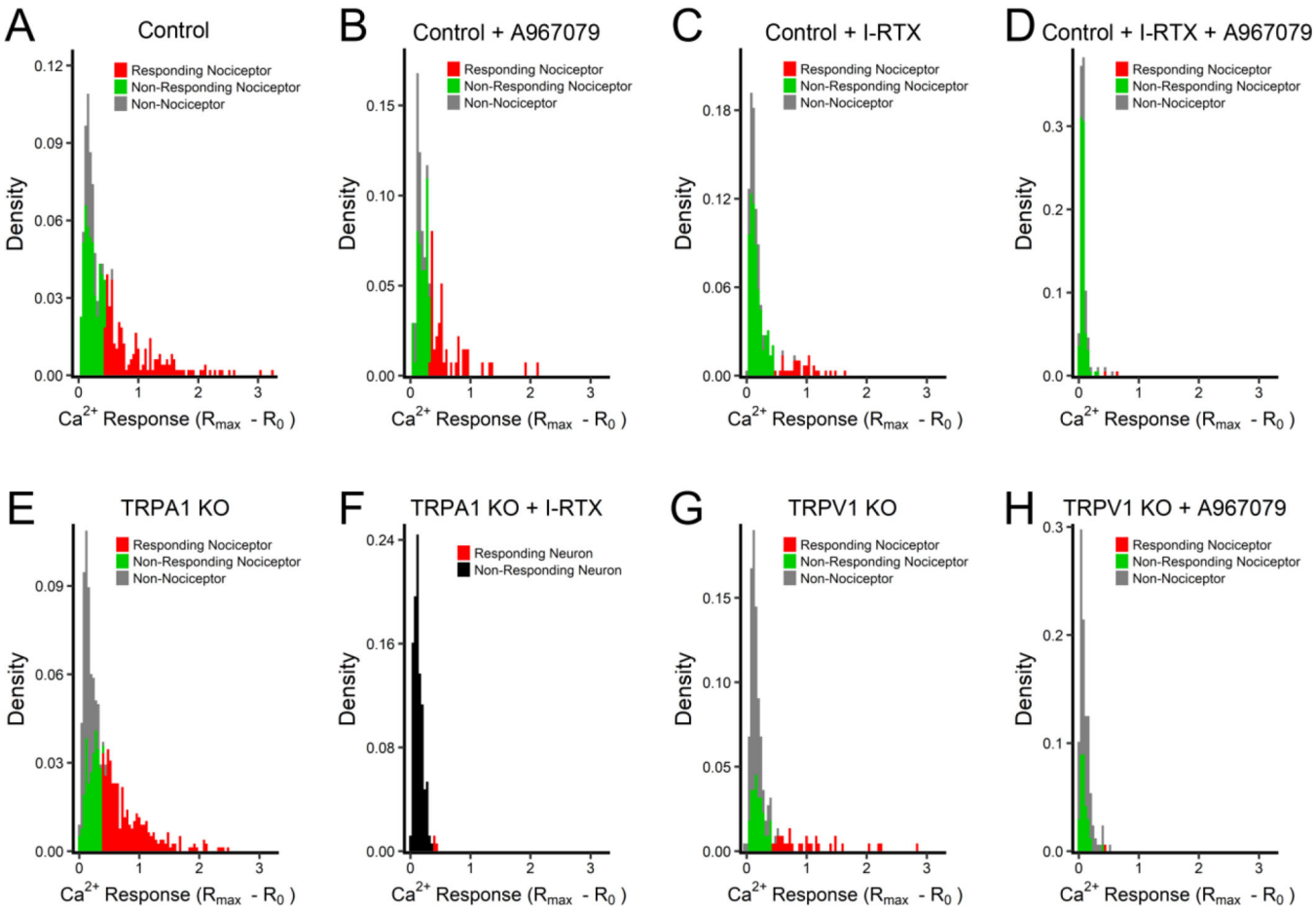

Fig 4:

Histograms of maximal antimycin A-evoked Ca2+ responses in vagal sensory neurons. A, TRPV1$^{Cre/+}$/ROSA26-tdTomato$^{fl/+}$ neurons (Control). B, Control neurons pretreated with A967079 (5μM). C, Control neurons pretreated with I-RTX (500nM). D, Control neurons pretreated with A967079 and I-RTX. E, TRPA1−/− neurons. F, TRPA1−/− neurons pretreated with I-RTX. G, TRPV1−/− neurons. H, TRPV1−/− neurons pretreated with A967079. In A–E and G–H, Non-nociceptor in grey columns, non-responding nociceptor in green, responding nociceptor in red. In F, non-responding neuron in black, responding neuron in red.

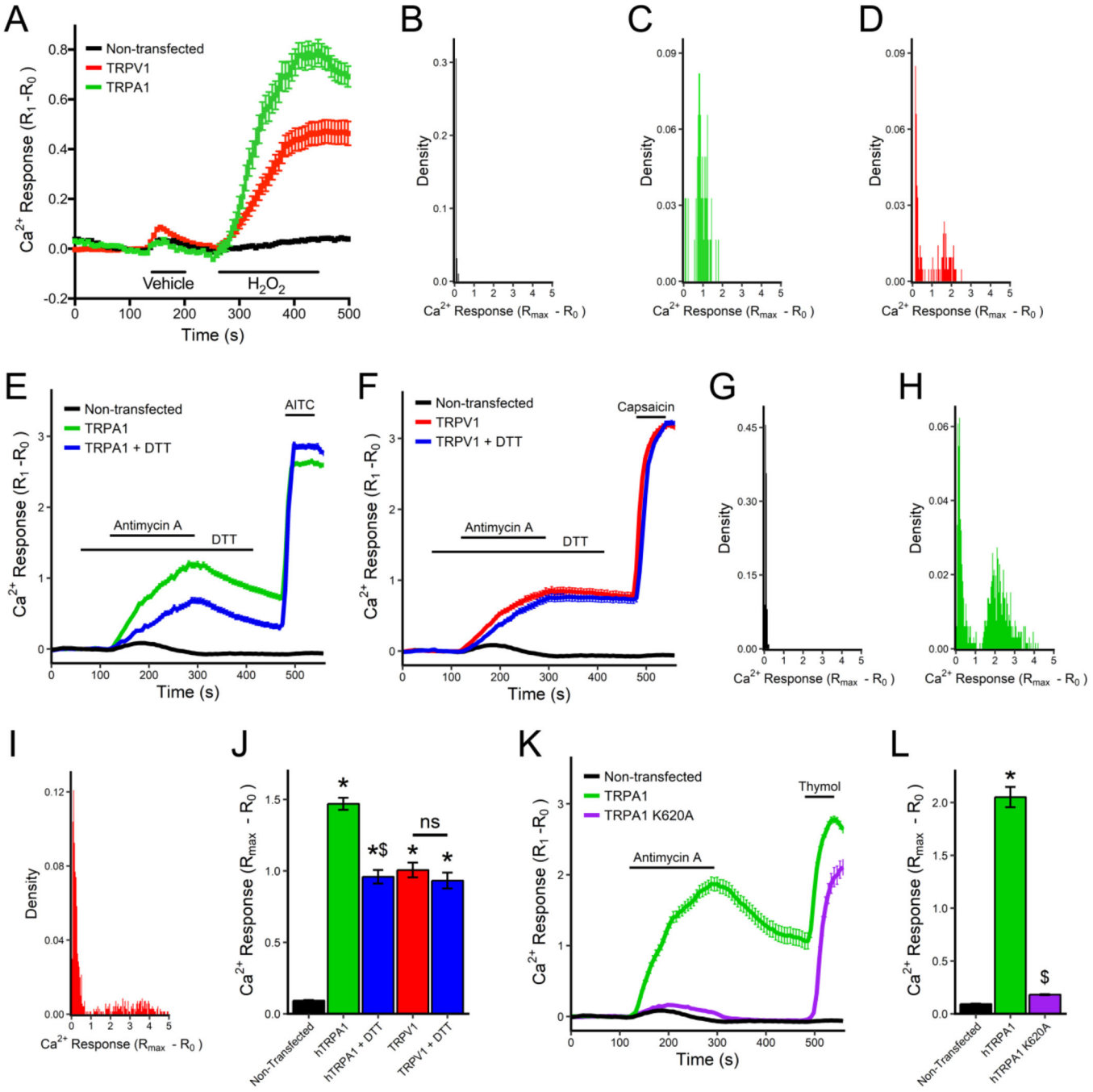

Fig 5:

Antimycin A activates hTRPA1 but not hTRPV1 by ROS-dependent mechanisms in HEK293 cells. A, Mean +/− SEM $[Ca^{2+}]_i$ responses to vehicle and H_2O_2 (100μM) in non-transfected (black line), hTRPA1-expressing (green line) and hTRPV1-expressing HEK293 cells (red line). B–D, Histograms of maximal H_2O_2-evoked Ca^{2+} responses in non-transfected HEK293 (B) and HEK293 transfected with hTRPA1 (C) or hTRPV1 (D). E, Mean +/− SEM $[Ca^{2+}]_i$ responses to antimycin A (10μM) and AITC (100μM) of non-transfected HEK293 (black line), and hTRPA1-expressing HEK293 with (blue line) and

without (green line) pretreatment with DTT (100μM). F, Mean +/− SEM $[Ca^{2+}]_i$ responses to antimycin A (10μM) and capsaicin (1μM) of non-transfected HEK293 (black line), and hTRPV1-expressing HEK293 with (blue line) and without (red line) pretreatment with DTT (100μM). G–I, Histograms of maximal antimycin A-evoked Ca^{2+} responses in non-transfected HEK293 (G) and HEK293 transfected with hTRPA1 (H) or hTRPV1 (I). J, Mean maximal $[Ca^{2+}]_i$ response to antimycin A in non-transfected HEK293, or HEK293 transfected with either hTRPA1 or hTRPV1 with or without DTT pretreatment. K, Mean +/− SEM $[Ca^{2+}]_i$ responses to antimycin A (10μM) and thymol (200μM) of HEK293 expressing wild-type hTRPA1 (green line) or the hTRPA1-K620A mutant (purple line). L, mean maximal $[Ca^{2+}]_i$ response to antimycin A in non-transfected HEK293, or HEK293 transfected with either hTRPA1 or hTRPA1-K620A. * denotes significant difference to non-transfected HEK293 responses ($p<0.05$), $ denotes significant difference to wild-type TRP responses ($p<0.05$), ns denotes no significant difference.

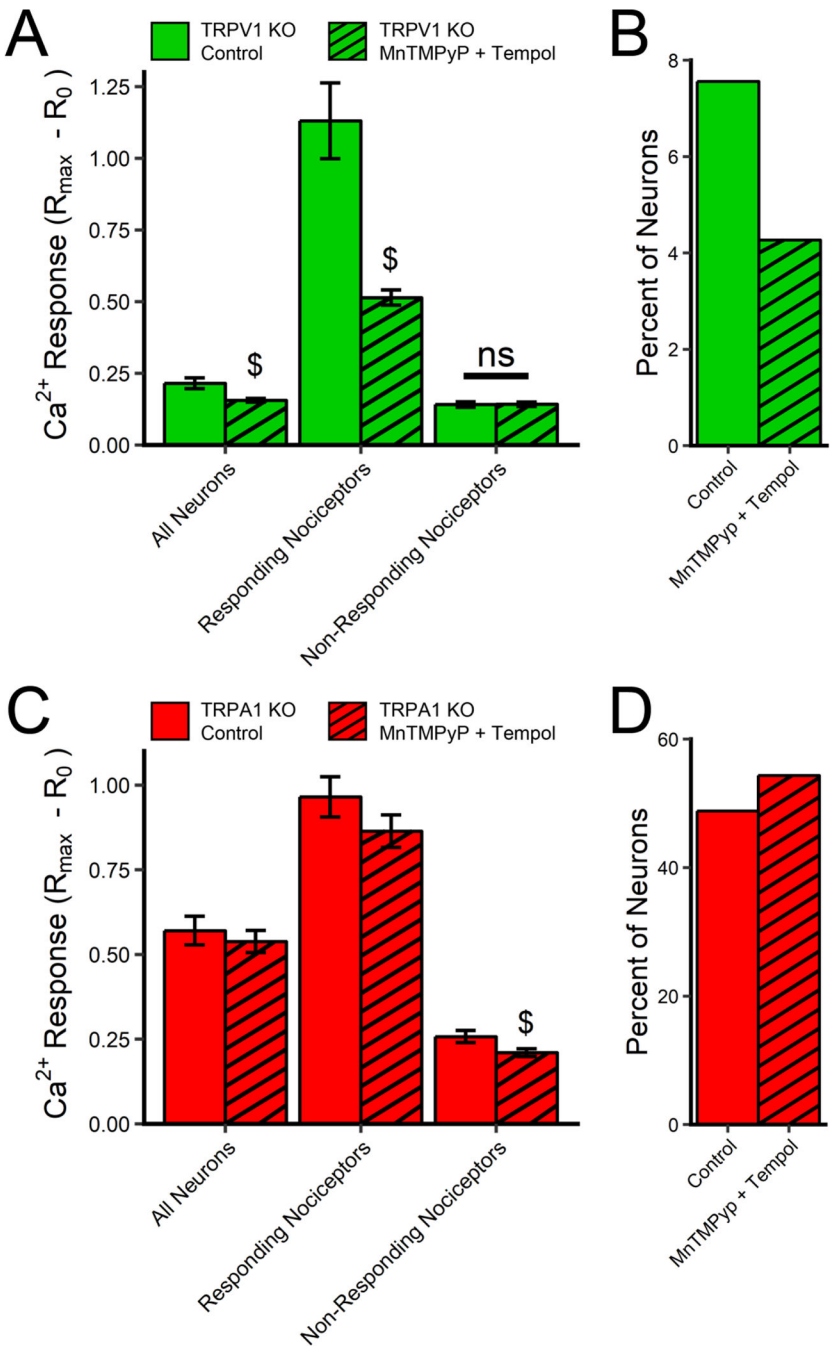

Fig 6:

ROS scavengers inhibit antimycin A-evoked Ca2+ responses mediated by TRPA1 but not TRPV1 in vagal sensory neurons. Responses to antimycin A (10μM) in vagal neurons from TRPV1−/− mice (green columns, in A and B) and TRPA1−/− mice (red columns, in C and D) with (hatched columns) and without (clear columns) pretreatment with MnTMPyP (50 μM) and tempol (100 μM). A and C, Mean maximal $[Ca^{2+}]_i$ responses to antimycin A of all neurons, responding nociceptors and non-responding nociceptors. B and D, percentage of all

neurons that responded to antimycin A. $ denotes significant difference to responses without ROS scavengers ($p<0.05$), ns denotes no significant difference.

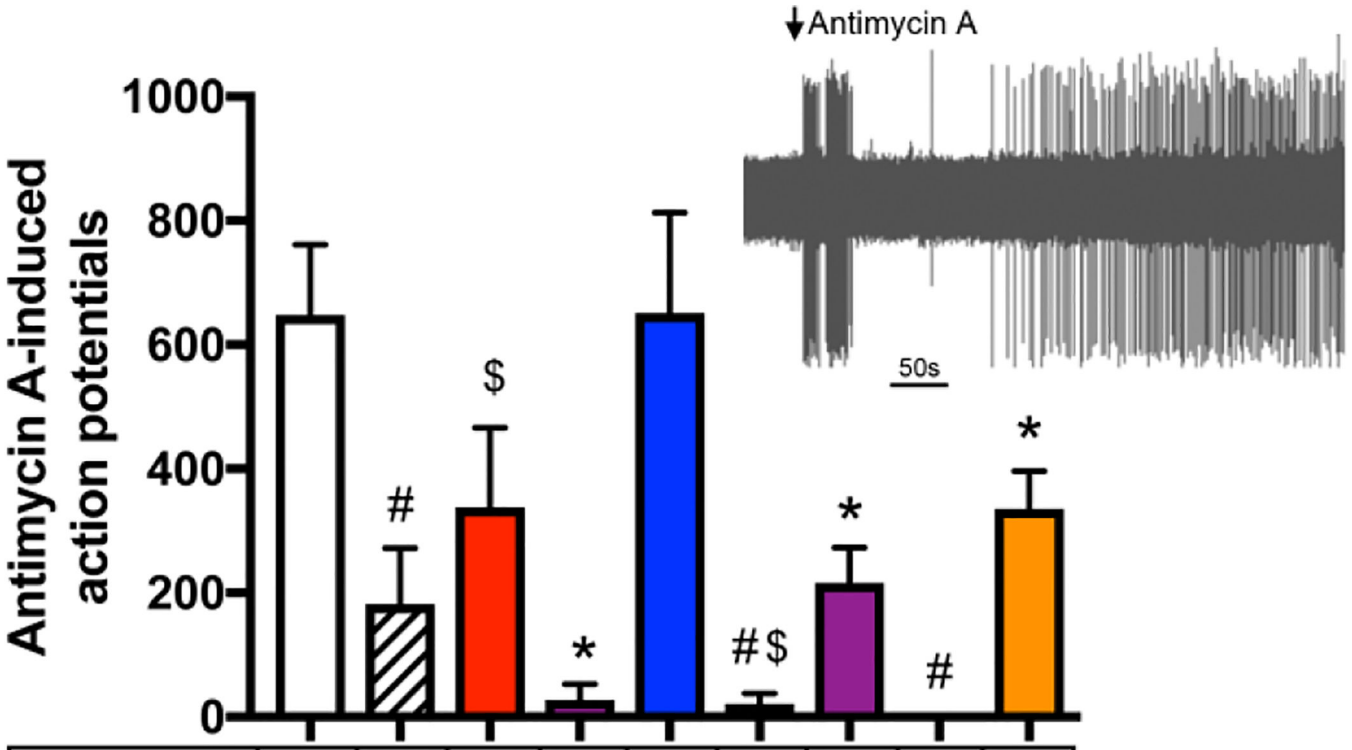

Strain	WT	WT	A1$^{-/-}$	A1$^{-/-}$	V1$^{-/-}$	V1$^{-/-}$	V1$^{-/-}$	V1$^{-/-}$	V1$^{-/-}$
Inhibitor				IRTX			A96	A96	anti-OX
AITC-sensitivity	Yes	No	n/a	n/a	Yes	No	Yes	No	Yes

Fig 7:

Antimycin A evokes action potential discharge from bronchopulmonary C-fibers via TRPA1 and TRPV1. Mean +/− SEM action potential discharge to antimycin A (10μM) from slowly-conducting bronchopulmonary C-fibers ex vivo. C-fibers from wild-type C57BL/6J mice, TRPA1−/− and TRPV1−/− were characterized by their sensitivity to AITC (30 μM). Some fibers were pretreated with either I-RTX (1 μM) or A967079 (A96, 30 μM) or a combination (anti-OX) of MnTMPyP (50 μM) and tempol (100 μM). # denotes significant difference between AITC-sensitive and AITC-insensitive fibers ($p<0.05$), $ denotes significant effect of the genetic knockout ($p<0.05$), * denotes significant of the inhibitor ($p<0.05$).